This article has been accepted for publication in a future issue of this journal, but has not been fully edited. Content may change prior to final publication. Citation information: DOI 10.1109/TIA.2019.2897947, IEEE Transactions on Industry Applications

Improvement of Stability margin of Droop based Islanded Microgrids by Cascading of Lead Compensators

Dharmendra Kumar Dheer, *Student Member, IEEE,* Vijay A S, Onkar Vitthal Kulkarni, *Student Member, IEEE,* and Suryanarayana Doolla*, *Senior Member, IEEE*

***Abstract*—Microgrids are systems consisting of local generators based on renewable energy sources, energy storage elements and loads. Such systems can be operated in grid connected and/or islanded modes. The islanded mode of operation is known to offer challenges in terms of stability. The work presented in this paper demonstrates a technique to enhance the stability margin of an islanded AC microgrid. Lead compensators are cascaded in series in the real power-frequency droop control of the distributed generators. This modification results in increased stability margin of the system. The work also investigates the possible limit upto which the stability margin can be increased. The effectiveness of the proposed technique is demonstrated through eigenvalue analysis and simulations on two systems: a low voltage islanded microgrid (system-1) and the islanded IEEE 33 bus system (system-2). Experimental results on a laboratory scale microgrid confirm the findings of the proposed strategy.**

***Index Terms*—Dynamic stability, microgrid, modified droop controls, small signal stability, stability margin, voltage source inverter.**

I. Introduction

Increasing demand of electrical energy, limited availability of conventional electrical energy sources and issues related to conventional sources on environment pollution creates the need for renewable energy sources integration into the conventional electrical power system. The integration of renewable sources is typically done at the distribution level at consumer end and termed as distributed generation (DG). The integration of different renewable energy sources like solar, wind, geothermal, biomass etc. as DGs, loads and energy storage devices give rise to the concept of a microgrid. A microgrid is capable of operating in grid connected mode, islanded mode or during transition [1]. The stability of the microgrid depends upon the control technique applied to the microsources and hence, a brief literature on control and stability of islanded microgrid is presented in this section. The research gap and the contribution are also highlighted.

In the grid connected operation of microgrid, DGs operate in the power control mode in which, operating frequency and voltage of the DGs are controlled by the main grid. In case of the islanded operation of the microgrid, voltage and frequency of the DGs are controlled by either centralized control scheme (master slave control), distributed control scheme or decentralized control scheme (droop control) [2]-[3]. Conventional droop control was first applied [4], for the islanded operation of uninterruptable power systems to control the frequency and voltage in parallel connected voltage source inverters. The control is based on the local measurements which is easy to implement, reliable and cost effective. Due to several issues (eg., unproportional reactive power sharing, slow transient response, poor performance in unbalanced and harmonic load conditions etc., [5]-[6]) associated with the implementation of conventional droop in low voltage microgrid, several modifications in the droop control have been proposed in the literature [2]-[3], [7]-[9].

The recent trend suggests an increase in the integration of inverter based sources into the microgrid. The droop based islanded microgrid with inverter based sources suffers from the small signal stability problem [10]-[13]. Several modifications to improve the stability margin of such a microgrid have been reported [14]-[22]. Increasing the stability margin by implemention of the supplementary and virtual impedance droop control are proposed in [17] and [18] respectively. In [19], a lead-compensator based modified droop control is proposed to enhance the stability margin of the microgrid. At higher loading conditions, improvement in the stability margin by implementing the arc-tan power-frequency droop control is proposed in [20]. Stability margin enhancement by implementing the angle droop is proposed in [21], which is further improved in [22]. The optimal energy management strategy using stability constrained droop-control for an islanded microgrid is discussed in [23] with an objective to minimize fuel consumption. The stability of a microgrid with constant power loads (voltage regulators and rectifiers) is analysed using the participation approach in [24]. The stability investigation of microgrids consisting of both diesel generators and inverters is discussed in [25]. Various efforts such as a decentralized cooperative control approach [26] for the autonomous operation mode, use of a large signal based control topology in the DGs for stabilization [27] in both grid connected and islanded modes, an adaptive feedforward compensation based approach [28] which ensures robust operation, a gain-scheduled decoupling control [29] for an islanded active distribution network, a supplementary controller in the photovoltaic (PV) control loop [30] for stability enhancement have been proposed by various researchers. Some of the other recent attempts to enhance stability in microgrids have been discussed in [31]-[41].

This paper mainly discusses about the enhancement of the stability margin in droop control based DGs for an

*Corresponding author: Suryanarayana Doolla (email: suryad@iitb.ac.in)

This article has been accepted for publication in a future issue of this journal, but has not been fully edited. Content may change prior to final publication. Citation information: DOI 10.1109/TIA.2019.2897947, IEEE Transactions on Industry Applications

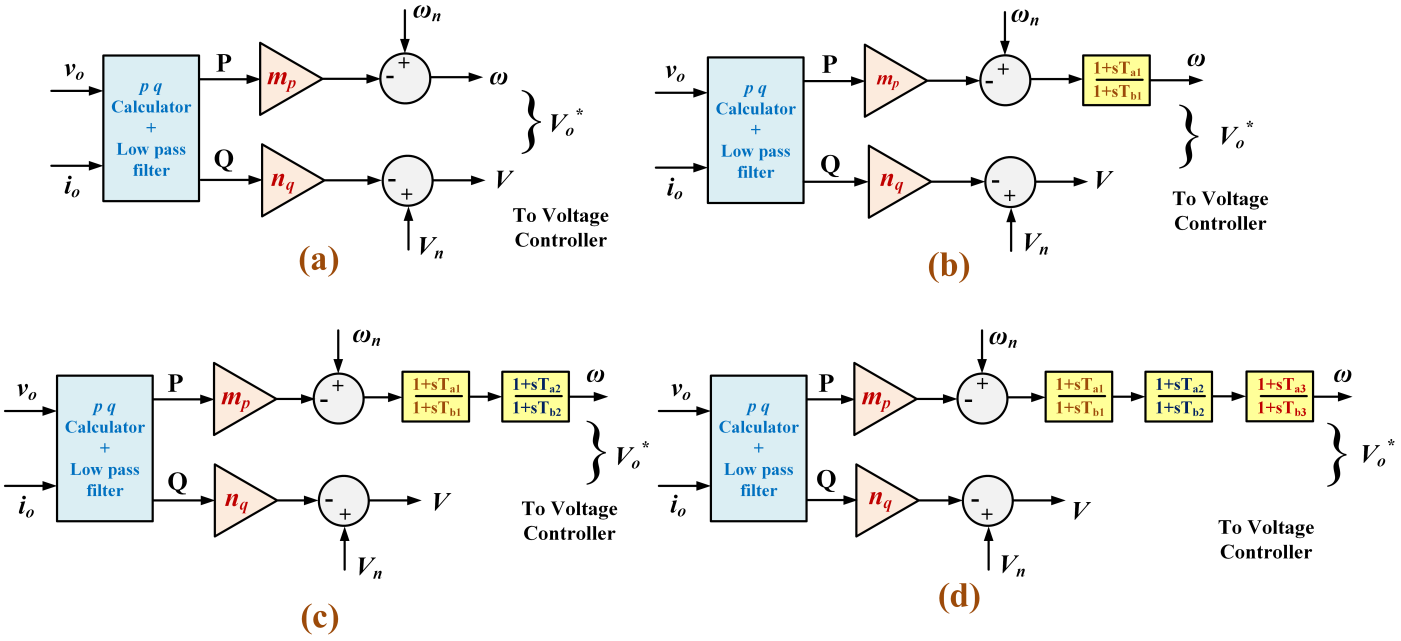

Fig. 1. Droop control modifications by cascading lead compensators: a) Conventional droop b) Modified droop-1 c) Modified droop-2 d) Modified droop-3

AC microgrid in the islanded mode. A comparative stability analysis for some of the popular droop control techniques has been carried out in [42], which reports that the stability margin is the highest for the modified droop-1 compared to the other three droop techniques : conventional droop control, generalized droop control and the virtual impedance based droop control. Even in the case of heterogeneous/mixed droop controllers, i.e different inverters of a system operating with different droop control schemes, it was found that the combinations with the modified droop-1 technique had higher stability margins compared to other combinations. Although the stability margin is increased by use of lead compensators in [19], the maximum possible stability margin which can be achieved by further modification in power-frequency droop has not been investigated. The contributions of this paper are twofold: the lead-compensator based modified droop control is further modified to obtain the maximum possible stability margin that can be achieved. The paper also reports the number of lead-compensators beyond which, the further cascading of such lead-compensators in the power-frequency droop does not bring a significant improvement in the stability margin of the system. The paper is organised as follows: section-II presents mathematical modeling and system description, section-III presents eigenvalue analysis, traces and discussion. Section-IV presents the simulation studies, section-V presents the experimental validation of the proposed modified droop control and section-VI presents the discussion and conclusions.

II. Mathematical Modeling and System Description

A generalised mathematical model of the voltage source inverter (VSI) based microgrid operating in the conventional and modified droop techniques is presented in this section. To compare the effect of the modified droops on the stability margin, a 220 V (V_{ph} rms), 50 Hz low voltage system and the standard IEEE 33-bus islanded system are considered which have been described below.

A. Mathematical modeling

In this sub-section modified droop controls are proposed by cascading lead compensators. The conventional droop Eq.(1) and the modified droop-1 Eq.(2) are available in literature [4] and [19] respectively. The droop control technique is further modified by cascading two more lead compensators (Modified droop-2 and 3, Eq. (3) and (4) respectively to enhance the stability margin of the system. The conventional frequency-active power (ω-P) droop and the modified droop techniques are as follows:

Conventional droop:

$$\omega = \omega_n - m_p P \tag{1}$$

Modified droop-1:

$$\omega = \frac{1+sT_{a1}}{1+sT_{b1}}(\omega_n - m_p P) \tag{2}$$

Modified droop-2:

$$\omega = \frac{1+sT_{a1}}{1+sT_{b1}}\frac{1+sT_{a2}}{1+sT_{b2}}(\omega_n - m_p P) \tag{3}$$

Modified droop-3:

$$\omega = \frac{1+sT_{a1}}{1+sT_{b1}}\frac{1+sT_{a2}}{1+sT_{b2}}\frac{1+sT_{a3}}{1+sT_{b3}}(\omega_n - m_p P) \tag{4}$$

where, ω_n is nominal frequency, ω is system frequency, P is active power output and m_p is ω-P droop coefficient respectively. T_{a1} and T_{b1} are time constants of the first lead compensator, T_{a2} and T_{b2} are time constants of the second lead

This article has been accepted for publication in a future issue of this journal, but has not been fully edited. Content may change prior to final publication. Citation information: DOI 10.1109/TIA.2019.2897947, IEEE Transactions on Industry Applications

compensator and T_{a3} and T_{b3} are time constants of the third lead compensator respectively. The proposed modifications are shown in Fig. 1. To achieve proportional reactive power sharing among sources, the conventional voltage-reactive power (V-Q) droop is applied which is given as:

$$v_{od}^{*} = V_n - n_q Q, \quad v_{oq}^{*} = 0 \tag{5}$$

where, v_{od}^{*} and v_{oq}^{*} are reference d and q-axis output voltages, V_n is the nominal voltage applied to the system, n_q is the V-Q droop coefficient and Q is the output reactive power of the source. In the case of $Q-V$ droop, high values of n_q increase the accuracy in the proportional reactive power sharing among the sources. Since the voltage is a local quantity (voltage at a given node is influenced by the local network parameters and load conditions), even for higher values of n_q, errors in reactive power sharing cannot be reduced beyond a certain limit. Additionally, a large values of n_q may result in occurrence of under-voltage in the system. Hence, to obtain the maximum permissible value of n_q is not of much interest to the researcher. Even from the point of view of stability the effect of the n_q droop gain is lesser than that of m_p droop gain [43]. Hence, in all the proposed droop controls no modification is made in the $Q-V$ droop control of the power controller.

Mathematical modeling (in the dq reference) of each inverter, line and load is obtained in individual synchronous rotating reference frames and then are translated onto a common reference to obtain the combined model of the system. The modified droop-1 and mathematical modeling of voltage source inverter operating in the conventional droop control are adapted from [19] and [43] respectively. The model is obtained by linearizing the system about an equilibrium point. Introduction of cascaded lead compensators into the ω-P droop technique increases the number of states of the system. Number of states of the voltage source inverter operating in conventional droop, modified droop-1, 2 and 3 are 13, 14, 15 and 16 respectively.

The dynamic modeling is modified for each droop technique and the complete model is obtained which is given as:

$$\begin{bmatrix} \dot{X_{Inv}} \\ X_{Line} \\ X_{Load} \end{bmatrix} = A_{MG} \begin{bmatrix} X_{Inv} \\ X_{Line} \\ X_{Load} \end{bmatrix} \tag{6}$$

where, X_{Inv}, X_{Line} and X_{Load} are the states of all the inverters, lines and loads respectively in the system. A_{MG} is state space matrix of the complete system. Size of A_{MG} is different for all the techniques. Assuming that a microgrid consists of s sources, n lines, m nodes and p loads. Size of A_{MG} when the sources are operating in conventional droop is: $(13s+2n+2p) \times (13s+2n+2p)$, modified droop-1 is: $(14s+2n+2p) \times (14s+2n+2p)$, modified droop-2 is: $(15s+2n+2p) \times (15s+2n+2p)$ and modified droop-3 is: $(16s+2n+2p) \times (16s+2n+2p)$ respectively.

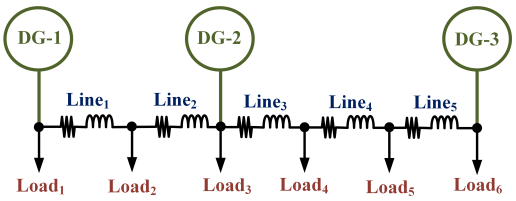

Fig. 2. System-1: Low voltage system

Table I
LINE AND LOAD DATA FOR SYSTEM 1

Line no.	Impedance	Load no.	Load
$Line_1$	(0.1+j0.08) Ω	$Load_1$	(2.5+j0.5) kVA
$Line_2$	(0.1+j0.12) Ω	$Load_2$	(1.0+j0.3) kVA
$Line_3$	(0.1+j0.15) Ω	$Load_3$	(5.0+j3.0) kVA
$Line_4$	(0.12+j0.15) Ω	$Load_4$	(1.5+j1.0) kVA
$Line_5$	(0.2+j0.25) Ω	$Load_5$	(1.0+j0.1) kVA
-	-	$Load_6$	(5.0+j1.0) kVA

B. System description

Two systems are considered to validate the claim of enhanced stability margin with the application of the proposed droop controls. System-1 is a low voltage microgrid network with three sources and system-2 is a standard islanded IEEE 33-bus network with three sources.

System-1: Low voltage microgrid: A low voltage microgrid under study is shown in Fig. 2. All the voltage source inverters are assumed of same rating (10 kVA, 220 V_{ph}). Line and load data are given in Table I.

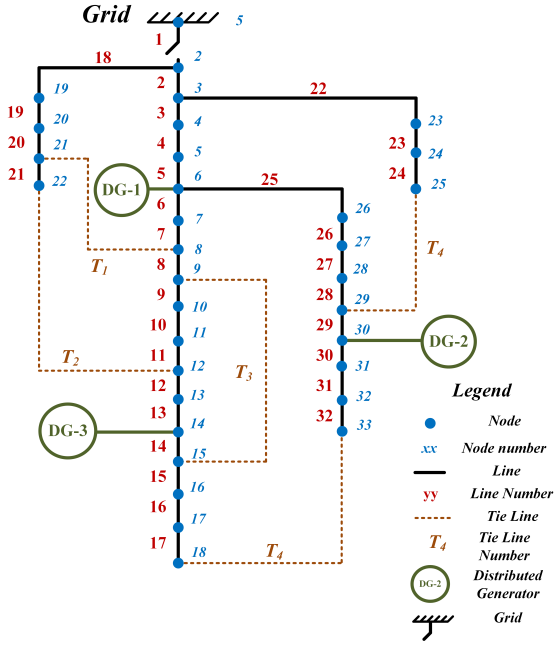

Fig. 3. System-2: The islanded IEEE 33-bus system

System-2: Standard IEEE 33-bus system: Fig. 3 shows the islanded IEEE 33 bus standard network with three sources.

This article has been accepted for publication in a future issue of this journal, but has not been fully edited. Content may change prior to final publication. Citation information: DOI 10.1109/TIA.2019.2897947, IEEE Transactions on Industry Applications

Line and load data of the network is adapted from [44]. In Fig. 3 the line numbers are marked on the right side of the line while the node numbers are marked on the left side of the node. The location and size of the sources are adapted from [45]. Sources connected at buses 6 (VSI-1), 14 (VSI-3) and 30 (VSI-2) share the power in proportion of 1.0:0.7:1.0 pu respectively.

III. Eigenvalue analysis, trace and discussion

Eigenvalue analysis is normally used to obtain the stability margin of the system [43], [45]-[52]. Since the system is non-linear, the small signal model of the system is developed by linearizing about an operating point. The system parameters at the operating point (equilibrium point) are obtained by simulating the system using Matlab Simulink. The values are then fed into a code which computes the eigenvalues of the system. It has been adequately reported in the literature [19],[43] that the low frequency modes of the system, corresponding to the power controller are most prone to instability. The real power droop gain m_p is therefore varied (increased in steps, iteratively in the code) and the trace of the eigenvalues is obtained (as given in Fig. 4 and 5 of the manuscript). The value of the droop coefficient at which the eigenvalues intersect the imaginary axis is then found, which is denoted as the small signal stability margin of the system (m_{p-max}). This process is repeated for all the proposed droop control techniques. It is to be noted that since the modification is made only in the power controller of the system, only the matrices corresponding to the small signal model of the power controller change, while the rest of the model remains the same. The detailed small signal modelling of complete system operating in modified droop-1 can be found in [19]. The Inverter parameters and the operating point values for modified droop-1, considered in the study for system 1 are presented in Table II and Table III respectively.

Table II
System 1 : Inverter (DG) parameters considered in simulation study

Parameter	Value	Parameter	Value
f_s	8 kHz	m_p	1×10^{-5} rad/s-W
L_f	1.8 mH	n_q	1×10^{-4} V/VAR
C_f	65 μF	K_{pv}	1
r_f	0.05 Ω	K_{iv}	0.32
L_c	0.33 mH	K_{pc}	0.001
r_{lc}	0.10 Ω	K_{ic}	1
ω_c	31.14 Hz	F	0.75
T_{a1}, T_{b1}	0.02, 0.0005	T_{a2}, T_{b2}	0.002, 0.00005
T_{a3}, T_{b3}	0.0002, 0.000005	V_n	380.0 V
Sampling time T_s	10μs	ω_n	314.159 rad/s

A. System-1: Low voltage system

Eigenvalues of the complete low voltage system are obtained for all the droop techniques. The m_p is taken 1.0×10^{-5} for all the cases. Effect of implementation of lead-compensator in the droop technique on the stability margin of the inverter based microgrid is investigated by varying the droop coefficient (m_p) applied to the inverters. Initial value of droop is taken 1×10^{-5} and it is increased in steps of 1×10^{-6} for all the droop techniques. Eigenvalue traces of the microgrid operating in conventional droop, modified droop-1, modified droop-2 and modified droop-3 with variation in droop gain (m_p) are shown in Fig. 4. λ_{12} and λ_{23} show the interaction of low frequency modes between inverters 1-2 and inverters 2-3. The stability analysis of the islanded microgrid was performed by changing the locations of the sources in [49] and it was found that the minimum line impedance between the sources has strong effect on the stability margin of the system. The network under study (Fig. 2) has three sources. The line impedance between DG-1 and DG-2 is (0.2+j0.2) Ω while the impedance between DG-2 and DG-3 is (0.42+j0.55) Ω. Due to the lesser line impedance between the sources 1 and 2, the low frequency modes associated with DG-1 and 2 (λ_{12}) goes into unstable mode before the low frequency modes associated with DG-2 and 3 (λ_{23}). This trend is observed in eigenvalue trace for all the droop techniques applied to the system.

Table III
System 1 : Operating points for Modified droop-1

Parameter	Value	Parameter	Value
V_{od1}, V_{od2}, V_{od3}	379.25, 377.5, 378 V	I_{lined1}, I_{lineq1}	8.23, -2.39 A
V_{oq1}, V_{oq2}, V_{oq3}	0, 0, 0 V	I_{lined2}, I_{lineq2}	5.62, -1.6 A
I_{od1}, I_{od2}, I_{od3}	13.45, 13.45, 13.45 A	I_{lined3}, I_{lineq3}	6.07, 0.0 A
I_{oq1}, I_{oq2}, I_{oq3}	-3.7, -6.3, -5.7 A	I_{lined4}, I_{lineq4}	2.17, 2.7 A
I_{ld1}, I_{ld2}, I_{ld3}	13.45, 13.45, 13.45 A	I_{lined5}, I_{lineq5}	-0.45, 3.0 A
I_{lq1}, I_{lq2}, I_{lq3}	-11.43, -14.03, -13.43 A	I_{loadd1}, I_{loadq1}	5.22, -1.31 A
V_{bd1}, V_{bd2}, V_{bd3}	377.75, 376.0, 376.5 V	I_{loadd2}, I_{loadq2}	2.61, -0.79 A
V_{bq1}, V_{bq2}, V_{bq3}	-7.5, -7.4, -6.8 V	I_{loadd3}, I_{loadq3}	13.0, -7.9 A
δ_1, δ_2, δ_3	0, 1.6×10^{-3}, -1.2×10^{-2} rad	I_{loadd4}, I_{loadq4}	3.9, -2.7 A
ω	314 rad/s	I_{loadd5}, I_{loadq5}	2.6, -0.27 A
		I_{loadd6}, I_{loadq6}	13.0, -2.7 A

Table IV
System-1: Eigenvalue trace analysis

S. no.	Droop Technique	$m_{p,max}$ (10^{-5})	Starting point	Intersection point on imaginary axis
1	Conventional	26.0	-9.422±j32.24	0± j50
2	Modified-1	50.4	-54.68±j72.0	0± j103.67
3	Modified-2	71.4	-54.58±j76.0	0± j124.0
4	Modified-3	75.2	-54.65±j76.3	0± j126.9

The stability margins ($m_{p,max}$) for all the droop techniques are obtained and are given in Table IV. From the eigenvalue trace it is found that introduction of lead compensator (modified droop-1) into the droop technique pushes the sensitive eigenvalues into the left half of the imaginary axis. The sensitive eigenvalue starts from (-9.422±j32.24) for the conventional droop which shifts towards left of the imaginary axis to (-54.68±j72.0) in the case of modified droop-1. The intersection points on imaginary axis also changes for the conventional droop (0± j50) and the modified droop-1 (0± j103.67) at which the system goes into unstable mode. The introduction of lead compensator (modified droop-1) into the conventional droop control technique increases the stability margin of the system from 26.0 $\times$ 10^{-5} to 50.7 $\times$ 10^{-5} (1.95 times approximately).

Further cascading of lead compensators as in the modified droop-2 and 3 techniques, does not push the sensitive eigenvalues to the left of the imaginary axis, but affects the movement

This article has been accepted for publication in a future issue of this journal, but has not been fully edited. Content may change prior to final publication. Citation information: DOI 10.1109/TIA.2019.2897947, IEEE Transactions on Industry Applications

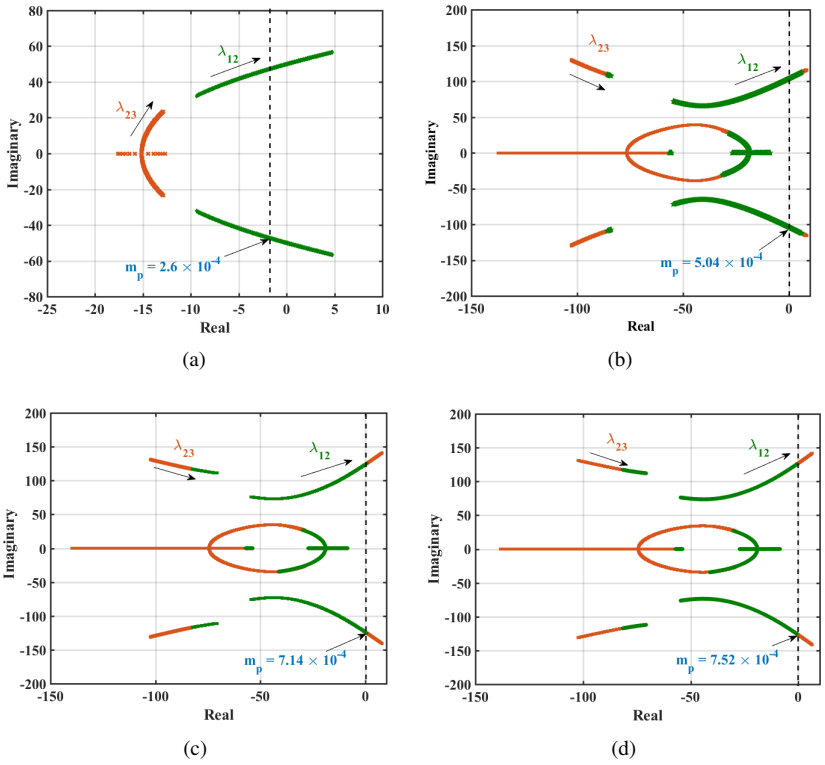

Fig. 4. System-1: Eigenvalue traces of microgrid operating in: a) conventional droop b) modified droop-1 c) modified droop-2 and d) modified droop-3 with variation in droop gain m_p

of the eigenvalues. Starting points of eigenvalues for the modified droop-1, 2 and 3 are (-54.68±j72.0), (-54.58±j76.0) and (-54.65±j76.3) respectively and the points on the imaginary axis at which the system goes into unstable mode are (0± j103.67), (0± j124.0) and (0± j126.9) respectively. In the case of modified droop-2, the change in the movement of eigenvalues (as compared to modified droop-1) is significant and hence, the stability margin increases from 50.7 $\times$ 10^{-5} to 71.4 $\times$ 10^{-5} (1.41 times approximately). Introduction of the third lead compensator into the droop technique (modified droop-3) has minimal effect on the movement of eigenvalues as compared to the modified droop-2 and hence, the increment in the stability margin is from 71.4 $\times$ 10^{-5} to 75.2 $\times$ 10^{-5} (1.05 times approximately) which is not too significant.

From the eigenvalue analysis and trace (for system-1: low voltage network) it is observed that a significant increment in the stability margin is obtained from the conventional droop to one lead compensator block addition (modified droop-1) which further increases with the second lead compensator block addition (modified droop-2). The addition of a third lead compensator (modified droop-3) does not significantly increase the stability margin of the system.

B. System-2: Standard IEEE 33-bus system

Eigenvalues for the complete 33 bus system is obtained for all the droop techniques. The effect of introduction of lead-compensators in the droop technique on the stability margin of the inverter based microgrid is investigated by varying the droop gain (m_p) applied to the inverters. The initial value of droop is taken 1.0 $\times$ 10^{-6} and it is increased in the steps of 2.0 $\times$ 10^{-7} for all the cases. The eigenvalue trace is performed to obtain the stability margin for all the droop techniques: conventional droop, modified droop-1, modified droop-2 and modified droop-3. The stability margins for all the droop techniques are given in Table V. The variation of the eigenvalue trace with the addition of lead compensators as given in the table clearly indicates that the trend observed in the IEEE 33-bus system is similar to that of the 3DG LV system (system-1). The only difference is that the addition of the third lead compensator block (modified-3 droop) in the control further increases the value at which the locus intersects with the imaginary axis, thus increasing the stability margin further when compared to the case in system-1, in which the addition of the third block did not increase the stability margin significantly.

Table V
SYSTEM-2: EIGENVALUE TRACE ANALYSIS

S. no.	Droop Technique	$m_{p,max}$ (10^{-6})	Starting point	Intersection point on imaginary axis
1	Conventional	18.1	-15.7±j6.205	0± j81.265
2	Modified-1	64.8	-195.4±j159.2	0± j334.2
3	Modified-2	167.0	-196.2±j160.1	0± j719.9
4	Modified-3	228.2	-197.2±j160.4	0± j981.2

Eigenvalue trace of the microgrid operating in all the droop techniques (conventional, modified-1, modified-2 and modified-3) are obtained. The eigenvalue traces of the microgrid operating in the various droop controls is as shown

This article has been accepted for publication in a future issue of this journal, but has not been fully edited. Content may change prior to final publication. Citation information: DOI 10.1109/TIA.2019.2897947, IEEE Transactions on Industry Applications

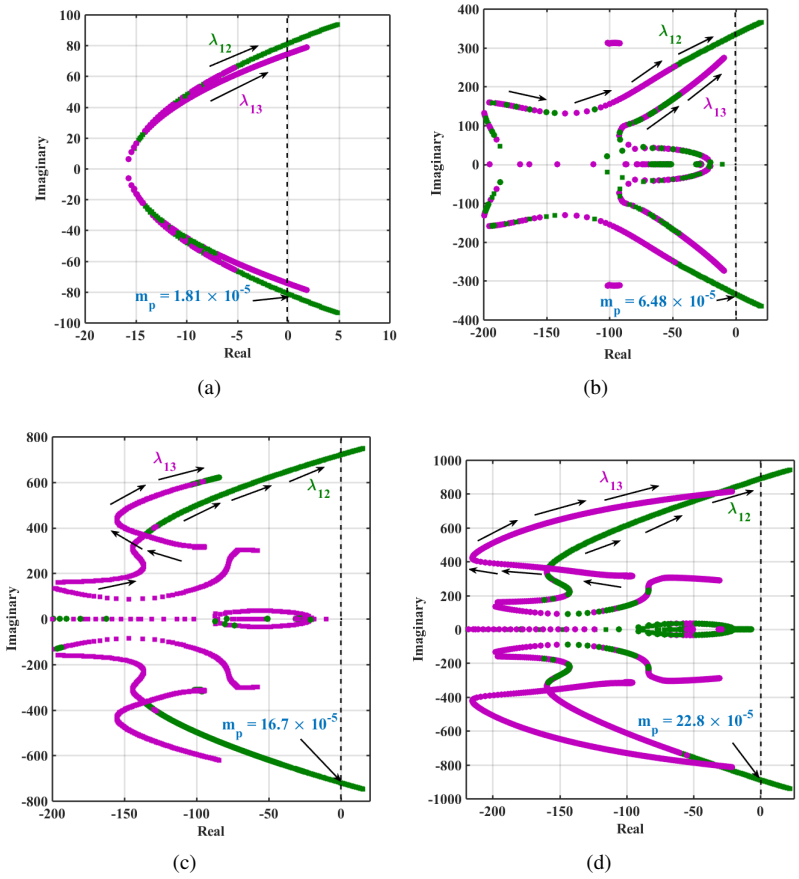

Fig. 5. System-2: Eigenvalue traces of microgrid operating in: a) conventional droop b) modified droop-1 c) modified droop-2 and d) modified droop-3 with variation in droop gain m_p

in Fig. 5. λ_{12} and λ_{13} show the interaction (participation factor analysis) of low frequency modes between inverters 1-2 and inverters 1-3 respectively. The modes associated with the power controller of voltage source inverters 1 and 2 goes into the unstable mode before as compared to the modes associated with the power controller modes of voltage source inverters 1 and 3. This trend is observed in the eigenvalue trace for all droop techniques applied to the system.

IV. Simulation Results and Discussion

The systems shown in Figs. 2 and 3 are simulated for two scenarios: to verify the power sharing among sources for the modified droop control techniques and to validate the results obtained through eigenvalue analysis.

A. System-1: Real power sharing

Time domain simulations in MATLAB for the low voltage microgrid with three sources (Fig. 2) is performed to verify the proportional power sharing among sources operating in conventional droop, modified droop-1, 2 and 3. At t = 2 s, a 3 kW load is connected in parallel with load_3 and active power output of all the three sources are plotted. Fig. 6 shows the active power output of the sources and the system frequency for the conventional droop control and for the modified droops 1, 2 and 3 respectively. All the sources are assumed of same rating (10 kVA) and hence, in each droop technique power sharing among sources are equal (for t $<$ 2s, $P_1 = P_2 = P_3$ = 5.33 kW, and for t $>$ 2s, $P_1 = P_2 = P_3$ = 6.33 kW).

B. System-1: Stability analysis

The effect of higher droop on stability is investigated by increasing the value of droop beyond the stability limit as shown in Table IV. For each droop technique, at t = 2s, the value of the droop coefficient is increased beyond the stability limit (conventional droop: $m_p >> 26.0 \times 10^{-5}$, modified droop-1: $m_p >> 50.4 \times 10^{-5}$, modified droop-2: $m_p >> 71.4 \times 10^{-5}$ and modified droop-3: $m_p >> 75.2 \times 10^{-5}$ respectively) and output current is plotted. Fig. 7 (a) shows the d-axis output current of DG-2 with the sources operating in conventional droop control. Beyond t = 2s, the currents starts oscillating which shows the unstable mode of operation. Figs. 7 (b) - (d) show the d-axis output current of DG-3 with the sources operating in modified droop-1, modified droop-2 and modified droop-3 respectively. In each modified droop technique it is found that the system goes into unstable mode beyond t = 2s (when m_p is increased beyond the margin). However the amplitude and nature of oscillation in the d-axis output current in the unstable mode are different from each other.

This article has been accepted for publication in a future issue of this journal, but has not been fully edited. Content may change prior to final publication. Citation information: DOI 10.1109/TIA.2019.2897947, IEEE Transactions on Industry Applications

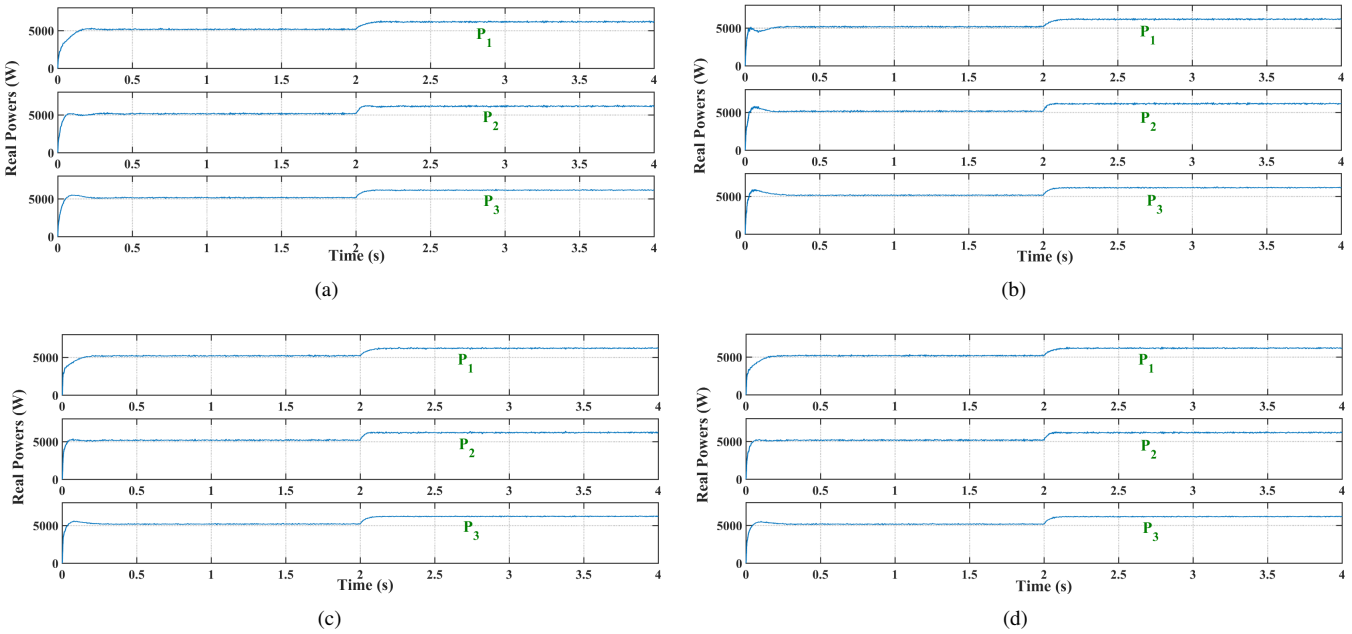

Fig. 6. System-1: Real power sharing among the sources: a) with conventional droop b) with modified droop-1 c) with modified droop-2 and d) with modified droop-3

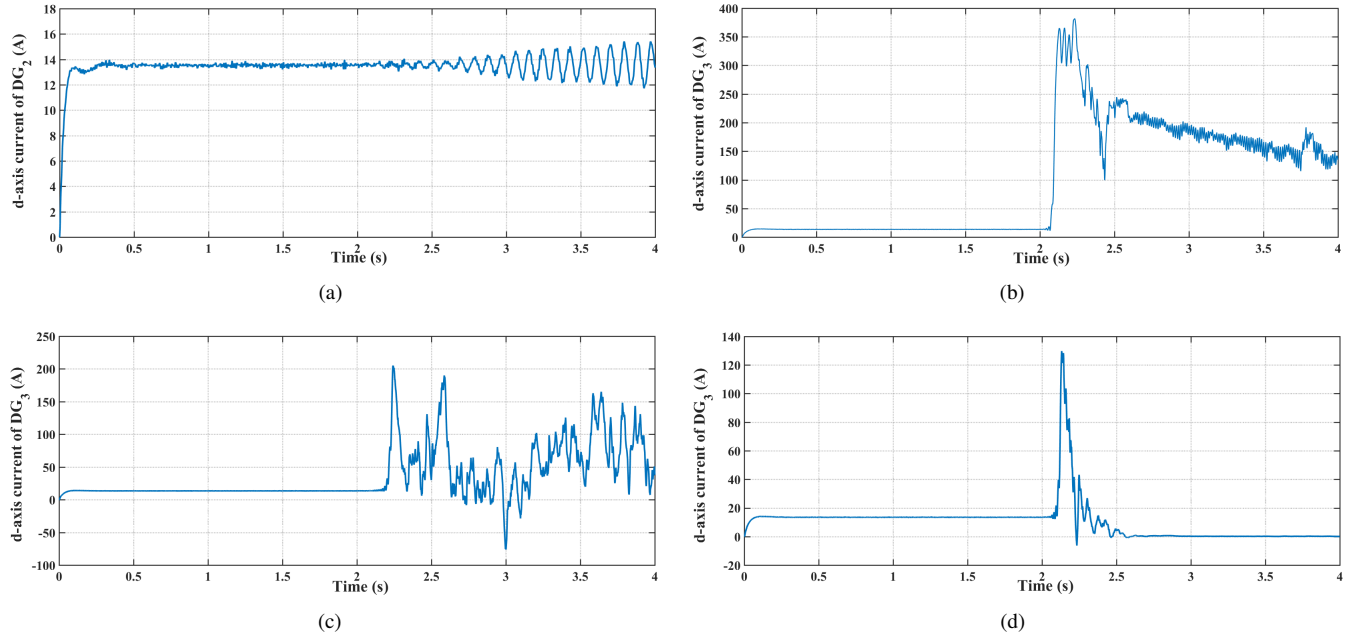

Fig. 7. System-1: d-axis output currents: a) of DG-2 with conventional droop b) of DG-3 with modified droop-1 c) of DG-3 with modified droop-2 and d) of DG-3 with modified droop-3 when when m_p is increased (beyond the respective stability limits) at t = 2s

C. System-2: Real power sharing

The time domain simulation in MATLAB for the standard IEEE 33-bus system with three sources (Fig. 3) is performed to verify the proportional power sharing among sources operating in conventional droop, modified droop-1, 2 and 3. Proportional power sharing among the sources operating in modified droop-2 (P_1 = 1.37 MW, P_2 = 1.37 MW, and P_3 = 0.96 MW) is shown in Fig. 8.

D. System-2: Stability analysis

The effect of higher droop on stability is investigated by increasing the value of droop beyond the stability limit as shown in Table V. For each droop technique, at t = 2s,the value of the droop coefficient is increased beyond the stability limit (conventional droop: $m_p >> 18.1 \times 10^{-6}$, modified droop-1: $m_p >> 64.8 \times 10^{-6}$, modified droop-2, $m_p >> 167.0 \times 10^{-6}$, modified droop-3, $m_p >> 228.2 \times 10^{-6}$) to verify the effect of higher droop on the system stability of the system. Fig. 9 shows the d-axis output current of DG-2 with the sources

This article has been accepted for publication in a future issue of this journal, but has not been fully edited. Content may change prior to final publication. Citation information: DOI 10.1109/TIA.2019.2897947, IEEE Transactions on Industry Applications

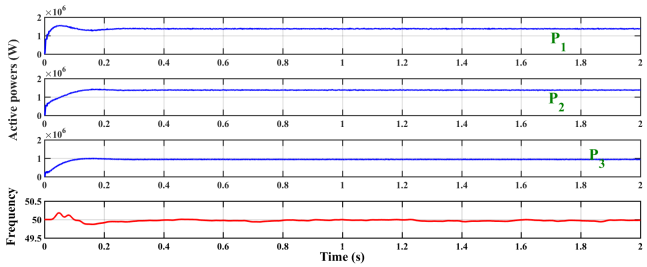

Fig. 8. System-2 (modified droop-2): Real power sharing among sources

operating in modified droop-2. At t= 2s, value of m_p is increased dynamically beyond it stability limit and the system goes into unstable mode.

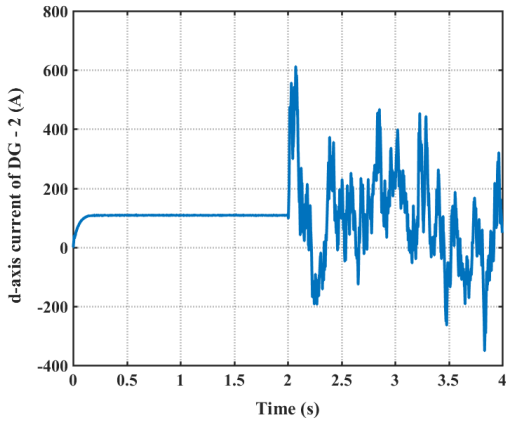

Fig. 9. System-2 (DGs operating in modified droop-2): d-axis output current of DG-2 when m_p is increased (beyond the stability limit) at t = 2s

V. Experimental Validation

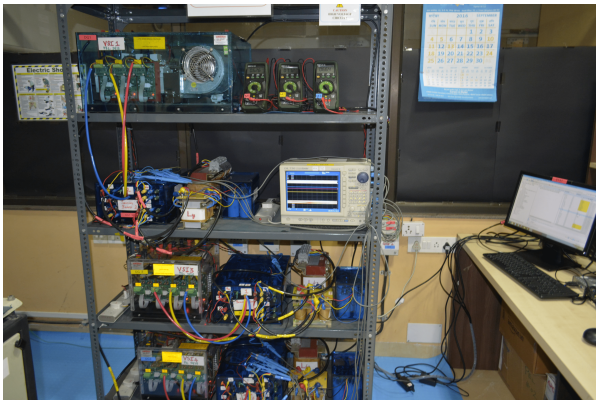

Fig. 10. Experimental setup in the laboratory

The simulation results are validated using a laboratory prototype as shown in Fig. 10. It consists of two equal rating inverter based DGs, three loads and interconnecting lines (realized using inductances) the parameters of which are mentioned in Table VI. The DC link voltages of these inverters are independently controlled using a dedicated three phase diode bridge rectifier connected to utility grid through

Table VI
Parameters in the Experimental Setup

Item	Symbol	Value
Filter inductor	L_f	1 mH
Filter capacitor	C_f	100 μF
Switching frequency	f_s	10 kHz
Nominal real power	P_o	500 W
Nominal reactive power	Q_o	75 VAR
Nominal output voltage	V_n	90 V (l-n)
Nominal frequency	ω_n	314.159 rad/s
Reactive power droop	n_q	0.01 V/var
Cut-off frequency (power controller filter)	ω_c	5 Hz
Proportional gain (voltage)	K_{pv}	1.0
Integral gain (voltage)	K_{iv}	0.5
Proportional gain (current)	K_{pv}	0.01
Integral gain (current)	K_{iv}	0.1
Lead Compensator Time constants (Block 1)	T_{a1}, T_{b1}	0.02, 0.0005
Lead Compensator Time constants (Block 2)	T_{a2}, T_{b2}	0.002, 0.00005
Sampling time	T_s	50μs

autotransformer for each inverter. Both the inverters operate in droop control mode using cascaded outer voltage and inner current control loop structure using TMS320F28335 floating point DSPs. The output AC voltage of the system is 90V (l-n rms) at the load side and at 50 Hz (DG output voltage stepped up using a 1:3 star connected transformer). Three cases are considered for the study: both the inverters operated under conventional droop control (case-1), both the inverters operated under modified-1 droop control (case-2) and both the inverters operated under modified-2 droop control (case-3). Since the addition of a third lead compensator does not improve the stability margin significantly and would involve a very small time step (practical implementation issues) it was not implemented in the experimental setup. The three-phase DG output voltages and active power waveforms of the two inverters operating in droop control mode are shown in Fig. 11. When all the inverters are having same droop coefficients ($m_p = 0.001$ rad/s/W), it can be observed that inverters are sharing active power equally (total load of 300W, each DG outputs 150W).

For all the cases:

1) The de-energized network is realised by the starting up of individual inverters and their synchronization.
2) The complete system is de-energized before proceeding to next case study.
3) Small signal stability margin ($m_{p,max}$ subjected to system stability) is analysed by varying the droop parameter (m_p) from 0.001 rad/s/W till the onset of oscillations in the real power outputs of the DGs (the stability limit).

For the experimental low voltage microgrid, the trend observed for stability margin ($m_{p,max}$) from the experiments is as follows: for conventional droop control (case-1) is 0.0045 rad/s/W, for modified droop-1 (case-2) is 0.0055 rad/s/W, and for modified droop-2 (case-3) is 0.015 rad/s/W. The decreasing order of stability obtained is thus: case-3 more stable than case-2 and case-2 more stable than case-1. To observe the small signal instability (oscillation in output power) inverters are initially synchronised and operated at $m_p = 0.001$ rad/s/W. Then for both the inverters, the droop coefficient is increased

This article has been accepted for publication in a future issue of this journal, but has not been fully edited. Content may change prior to final publication. Citation information: DOI 10.1109/TIA.2019.2897947, IEEE Transactions on Industry Applications

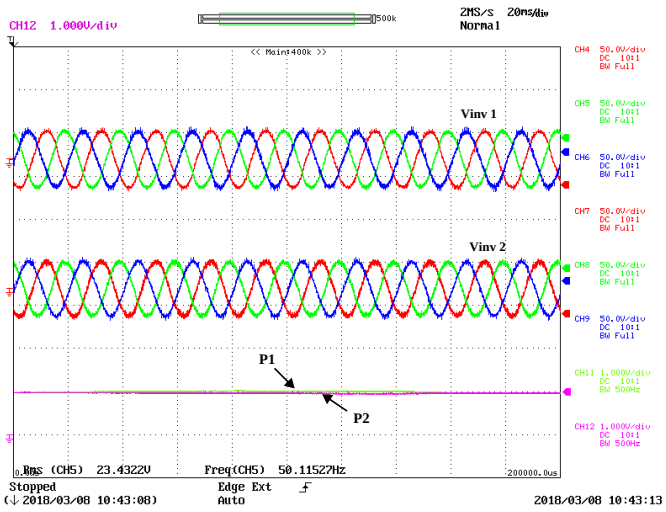

Fig. 11. Inverter Output phase voltages (DG side) and active powers for modified droop control case-2 at m_p of 0.001 rad/s/W (scales: voltage (50 V/div.), power (150 W/div.), time (20 ms/div.))

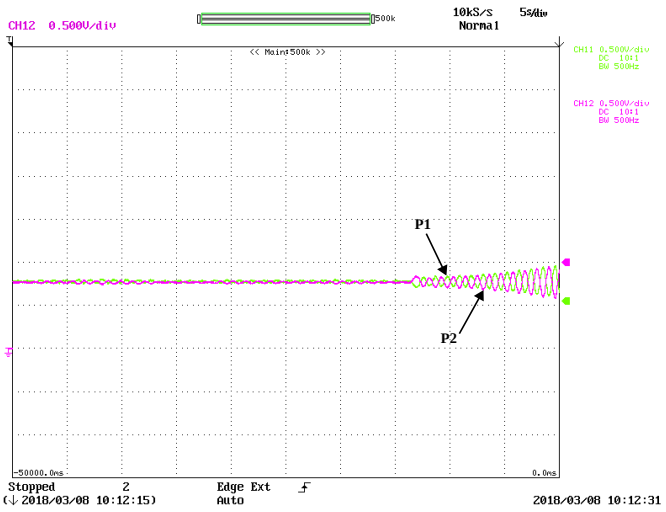

Fig. 13. Power sharing performance in modified droop-1, case-2: Oscillations when m_p is increased beyond 0.0055 rad/s/W (scale: power (75 W/div.), time (5 s/div.))

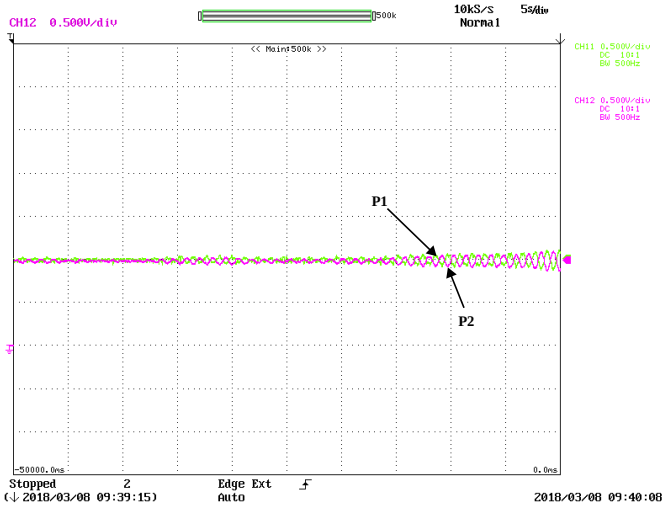

Fig. 12. Power sharing performance in conventional droop, case-1: Oscillations when m_p is increased beyond 0.0045 rad/s/W (scale: power (75 W/div.), time (5 s/div.))

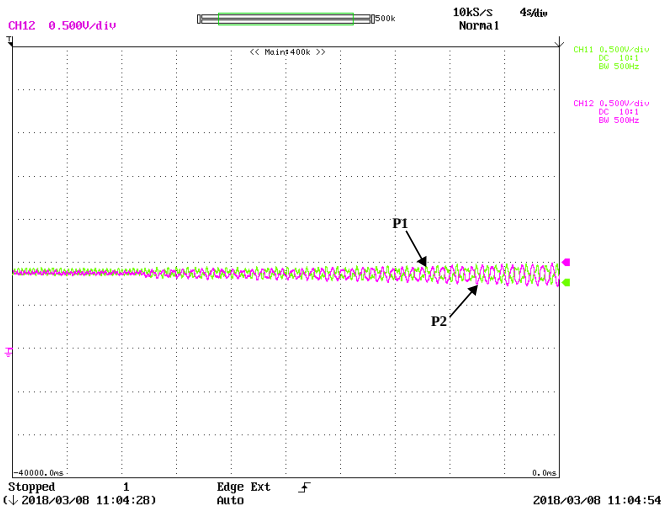

Fig. 14. Power sharing performance in modified droop-2, case-3: Oscillations when m_p is increased beyond 0.015 rad/s/W (scale: power (75 W/div.), time (5 s/div.))

in steps of $m_p = 0.0005$ rad/s/W, till the onset of oscillations in the output powers of the inverters. The effect of increasing the droop coefficients for both the inverters operated under the conventional and different modified droop control techniques are as shown in Fig. 12 - 14 respectively. It can be observed that the oscillations in the power sharing occur at increased values of droop coefficient with the addition of each lead compensator. Hence, it is experimentally verified that cascading of lead compensators increases the stability margin of the system.

VI. Discussion and Conclusion

The islanded mode of operation of the microgrid offers challenges in terms of stability. Several modifications in the control of distributed sources have been proposed in the literature to increase the stability margin of such systems. The work presented in the paper, proposes modifications in the droop control by the cascading of lead compensators in the real power-frequency droop control for the enhancement of the stability margin of the system. A detailed study to derive the state space matrix of the system (modelling) and the and small signal stability analysis was carried out about the operating point and the eigenvalues are obtained. Eigenvalue traces considering the participation factors are plotted for investigating the effect of increased droop gain/coefficient on the stability, for the various proposed droop control modifications. From the eigenvalue analysis for both the systems considered for study in the work, it is found that a significant increment in stability margin is observed from the conventional droop with the cascading of lead compensators (two blocks). Further cascading of lead compensators (modified droop-2 to modified droop-3) does not significantly increase the stability margin of the system. Thus, the limit to which the stability margin can be increased by the cascading of lead compensators is also obtained. The observations from the analysis are verified using

time domain simulations in MATLAB/SIMULINK. Experimental verification of the proposed analysis and confirmation of the claims is done through testing on a small laboratory scale microgrid prototype.

ACKNOWLEDGEMENTS

The authors would like to thank the support of the Ministry of New and Renewable Energy (MNRE), India for funding under the National Centre for Photovoltaic Research and Education (NCPRE) - phase 2 project (project code: 16MNRE002) and the support from India-UK Centre for Education and Research in Clean Energy (IUCERCE), a project funded by Department of Science and Technology (DST), India.

REFERENCES

[1] J. M. Guerrero, P. C. Loh, T. L. Lee, and M. C. Chandorkar, "Advanced control architectures for intelligent microgrids-part II: power quality, energy storage, and AC/DC microgrids," *IEEE Trans. Ind. Electron.*, vol. 60, no. 4, pp. 1263-1270, Apr. 2013.

[2] D. E. Olivares, A. M. Sani, A. H. Etemadi, C. A. Canizares, R. Iravani, M. Kazerani, A. H. Hajimiragha, O. G. Bellmunt, M. Saeedifard, R. P. Behnke, G. A. J. Estevez, and N. D. Hatziargyriou, "Trends in microgrid control," *IEEE Trans. Smart Grid*, vol. 5, no. 4, pp. 1905-1919, Jul. 2014.

[3] J. M. Guerrero, M. C. Chandorkar, T. L. Lee, and P. C. Loh, "Advanced control architectures for intelligent microgrids-part I: decentralized and hierarchical control," *IEEE Trans. Ind. Electron.*, vol. 60, no. 4, pp. 1254-1262, Apr. 2013.

[4] M. C. Chandorkar, D. M. Diwan, and R. Adapa, "Control of parallel connected inverters in standalone AC supply systems," *IEEE Trans. Ind. Appl.*, vol. 29, no. 1, pp. 136-143, Jan./Feb. 1993.

[5] E. Alizadeh, A. M. Birjandi, and M. Hamzeh, "Decentralised power sharing control strategy in LV microgrids under unbalanced load conditions," *IET Gen. Trans. and Dist.*, vol. 11, no. 7, pp. 1613-1623, 2017.

[6] P. Sreekumar, and V. Khadkikar, "A new virtual harmonic impedance scheme for harmonic power sharing in an islanded microgrid," *IEEE Trans. Power Del.*, vol. 31, no. 3, pp. 936-945, Jun. 2016.

[7] B. M. Eid, N. A. Rahim, J. Selvaraj, and A. H. E. Khateb, "Control methods and objectives for electronically coupled distributed energy resources in microgrids: a review," *IEEE Syst. Jour.*, vol. 10, no. 2, pp. 446-458, Jun. 2016.

[8] U. B. Tayab, M. A. B. Roslan, L. J. Hwai, and M. Kashif, "A review of droop control techniques for microgrid," *Renewable and Sustainable Energy Reviews, Elsevier*, vol. 76, pp. 717-727, Sept. 2017.

[9] E. Planas, A. G. de Muro, J. Andreu, I. Kortabarria, and I. M. de Alegria, "General aspects, hierarchical controls and droop methods in microgrids: a review," *Renewable and Sustainable Energy Reviews, Elsevier*, vol. 17, pp. 147-159, Jan. 2013.

[10] D. K. Dheer, A. S. Vijay, O. V. Kulkarni, and S. Doolla, "Improvement of Stability margin of Droop based Islanded Microgrids by Cascading of Lead Compensators," *In Proc. IEEE IAS General Meeting, Portland, US*, 23-27 Sep. 2018.

[11] E. Rikos, S. Tselepis, C. H. Klick, and M. S. Homscheidt, "Stability and power quality issues in microgrids under weather disturbances," *IEEE J. Sel. Topics Appl. Earth Observ. in Remote Sens.*, vol. 1, no. 3, pp. 170-179, Sep. 2008.

[12] A. Adib, B. Mirafzal, X. Wang, and F. Blaabjerg, "On stability of voltage source inverters in weak grids," *IEEE Open Access*, vol. 6, pp. 4427-4439, Feb. 2018.

[13] M. F. M. Arani, and Y. A. R. I. Mohamed, "Analysis and impacts of implementing droop control in DFIG-based wind turbines on microgrid/weak-grid stability," *IEEE Trans. Power Syst.*, vol. 30, no. 1, pp. 385-396, Jan. 2015.

[14] R. Majumder, "Some aspects of stability in microgrids," *IEEE Trans. Power Syst.*, vol. 28, no. 3, pp. 3243-3252, Aug. 2013.

[15] S. Wang, J. Su, X. Yang, Y. Du, Y. Tu, and H. Xu, "A review on the small signal stability of microgrid," *In Proc. IEEE IPEMC-ECCE Asia*, pp. 1793-1798, 22-26 May 2016.

[16] Z. Shuai, Y. Sun, Z. J. Shen, W. Tian, Ch. Tu, Y. Li, and X. Yin, "Microgrid stability: classification and a review," *Renewable and Sustainable Energy Reviews, Elsevier*, vol. 58, pp. 167-179, 2016.

[17] R. Majumder, B. Chaudhuri, A. Ghosh, R. Majumder, G. Ledwich, and F. Zare, "Improvement of stability and load sharing in an autonomous microgrid using supplementary droop control loop," *IEEE Trans. Power Syst.*, vol. 25, no. 2, pp. 796-808, May 2010.

[18] J. He, and Y. W. Li, "Analysis, design, and implementation of virtual impedance for power electronics interfaced distributed generation," *IEEE Trans. Ind. Appl.*, vol. 47, no. 6, pp. 2525-2538, Nov./Dec. 2011.

[19] D. K. Dheer, N. Soni, and S. Doolla, "Improvement of small signal stability margin and transient response in inverter-dominated microgrids," *Sustainable Energy Grids and Networks, Elsevier*, vol. 5, pp. 135-147, Mar. 2016.

[20] C. N. Rowe, T. J. Summers, R. E. Betz, D. J. Cornforth and T. G. Moore, "Arctan power-frequency droop for improved microgrid stability," *IEEE Trans. Power Electron.*, vol. 28, no. 8, pp. 3747-3759, Aug. 2013.

[21] R. Majumder, G. Ledwich, A. Ghosh, S. Chakrabarti, and F. Zare, "Droop control of converter-interfaced microsources in rural distributed generation," *IEEE Trans. Power Del.*, vol. 25, no. 4, pp. 2768-2778, Oct. 2010.

[22] H. Moussa, A. Shahin, J. P. Martin, S. Pierfederici, and N. Moubayed, "Optimal angle droop for power sharing enhancement with stability improvement in islanded microgrids," *IEEE Trans. Smart Grid*, vol. 9, no. 5, pp. 5014-5026, Sep. 2018.

[23] E. Barklund, N. Pogaku, M. Prodanovic, C. H. Aramburo, and T. C. Green, "Energy management in autonomous microgrid using stability-constrained droop control of inverters," *IEEE Trans. Power Electron.*, vol. 23, no. 5, pp. 2346-2352, Sep. 2008.

[24] N. Bottrell, M. Prodanovic, Member, and T. C. Green, "Dynamic stability of a microgrid with an active load," *IEEE Trans. Power Electron.*, vol. 28, no. 11, pp. 5107-5119, Nov. 2013.

[25] Z. Miao, A. Domijan, Jr., and L. Fan, "Investigation of microgrids with both inverter interfaced and direct AC-connected distributed energy resources," *IEEE Trans. Power Del.*, vol. 26, no. 3, pp. 1634-1642, Jul. 2011.

[26] P. H. Divshali, A. Alimardani, S. H. Hosseinian, and M. Abedi, "Decentralized cooperative control strategy of microsources for stabilizing autonomous VSC-based microgrids," *IEEE Trans. Power Syst.*, vol. 27, no. 4, pp. 1949-1959, Nov. 2012.

[27] S. M. Ashabani and Y. A. I. Mohamed, "A flexible control strategy for grid-connected and islanded microgrids with enhanced stability using nonlinear microgrid stabilizer," *IEEE Trans. Smart Grid*, vol. 3, no. 3, pp. 1291-1301, Sep. 2012.

[28] M. B. Delghavi, and A. Yazdani, "An adaptive feedforward compensation for stability enhancement in droop-controlled inverter-based microgrids," *IEEE Trans. Power Del.*, vol. 26, no. 3, pp. 1764-1773, Jul. 2011.

[29] A. Haddadi, A. Yazdani, Geza Joos, and Benoit Boulet, "A gain-scheduled decoupling control strategy for enhanced transient performance and stability of an islanded active distribution network," *IEEE Trans. Power Del.*, vol. 29, no. 2, pp. 560-569, Apr. 2014.

[30] S. Mishra, and D. Ramasubramanian, "Improving the small signal stability of a PV-DE-dynamic load-based microgrid using an auxiliary signal in the PV control loop," *IEEE Trans. Power Syst.*, vol. 30, no. 1, pp. 166-176, Jan. 2015.

[31] J. Alipoor, Y. Miura, and T. Ise, "Stability assessment and optimization methods for microgrid with multiple VSG units," *IEEE Trans. Smart Grid*, vol. 9, no. 2, pp. 1462-1471, Mar. 2018.

[32] A. Aderibole, H. H. Zeineldin, M. S. El-Moursi, J. C. Peng, and M. Al Hosani, "Domain of Stability Characterization for Hybrid Microgrids Considering Different Power Sharing Conditions," *IEEE Trans. Energy Convers.*, vol. 33, no. 1, pp. 312-323, Mar. 2018.

[33] A. Bolzoni, G. M. Foglia, L. Frosio, M. F. Iacchetti, and R. Perini, "Impact of Line and Control Parameters on Droop Stability in Inverters for Distributed Generation," *IEEE Trans. Smart Grid*, vol. 9, no. 6, pp. 6656-6665, Nov. 2018.

[34] Z. Li, and M. Shahidehpour, "Small-Signal Modeling and Stability Analysis of Hybrid AC/DC Microgrids," *IEEE Trans. Smart Grid*, IEEE Early Access.

[35] Y. Pan, L. Chen, X. Lu, J. Wang, F. Liu, and S. Mei, "Stability Region of Droop-Controlled Distributed Generation in Autonomous Microgrids," *IEEE Trans. Smart Grid*, IEEE Early Access.

[36] Y. Yan, D. Shi, D. Bian, B. Huang, Z. Yi, and Z. Wang, "Small-signal Stability Analysis and Performance Evaluation of Microgrids under Distributed Control," *IEEE Trans. Smart Grid*, IEEE Early Access.

[37] L. B. G. Campanhol, S. A. O. Silva, A. A. O. Junior, and V. D. Bacon, "Power Flow and Stability Analyses of a Multifunctional Distributed Generation System Integrating a Photovoltaic System with Unified Power Quality Conditioner," *IEEE Trans. Power Electron.*, IEEE Early Access.

[38] A. Millner, S. Christopher, R. Jaddivada, and I. D. Marija, "Component Standards for Stable Microgrids," *IEEE Trans. Power Syst.*, IEEE Early Access.

[39] W. Cao, Y. Ma, L. Yang, F. Wang, and Leon M. Tolbert, "D–Q impedance based stability analysis and parameter design of three-phase inverter-based AC power systems," *IEEE Trans. Ind. Electron.*, vol. 64, no. 7, pp. 6017-6028, Jul. 2017.

[40] X. Wu, and C. Shen, "Distributed optimal control for stability enhancement of microgrids with multiple distributed generators," *IEEE Trans. Power Syst.*, vol. 32, no. 5, pp. 4045-4059, Sep. 2017.

[41] Y. Zhang, L. Xie, and Q. Ding, "Interactive control of coupled microgrids for guaranteed system-wide small signal stability," *IEEE Trans. Smart Grid*, vol. 7, no. 2, pp. 1088-1096, Mar. 2016.

[42] A. S. Vijay, D. K. Dheer, A. Tiwari, and S. Doolla, "Performance evaluation of homogeneous and heterogeneous droop based systems in microgrid-stability and transient response perspective," *IEEE Trans. Energy Convers.*, IEEE Early Access.

[43] N. Pogaku, M. Prodanovic, and T. C. Green, "Modeling, analysis and testing of autonomous operation of an inverter-based microgrid," *IEEE Trans. Power Electron.*, vol. 22, no. 2, pp. 613-625, Mar. 2007.

[44] B. Venkatesh, R. Ranjan, and H. B. Gooi, "Optimal reconfiguration of radial distribution systems to maximize loadability," *IEEE Trans. Power Syst.*, vol. 19, no. 1, pp. 260-266, Feb. 2004.

[45] D. K. Dheer, O. V. Kulkarni, S. Doolla, and A. K. Rathore, "Effect of reconfiguration and meshed networks on small signal stability margin of droop-based islanded microgrids," *IEEE Trans. Ind. Appl.*, vol. 54, no. 3, pp. 2821-2823, May/Jun. 2018.

[46] X. Tang, W. Deng, and Z. Qi, "Investigation of the dynamic stability of microgrid," *IEEE Trans. Power Syst.*, vol. 29, no. 2, pp. 698-706, Mar. 2014.

[47] S. Leitner, M. Yazdanian, A. M. Sani, and A. Muetze, "Small-signal stability snalysis of an inverter-based microgrid with internal model-based controllers," *IEEE Trans. Smart Grid*, vol. 9, no. 5, pp. 5393-5402, Sep. 2014.

[48] D. K. Dheer, N. Soni, and S. Doolla, "Small signal stability in microgrids with high penetration of power electronics interfaced sources," *In Proc. IEEE IECON*, pp. 2272-2278, Oct./Nov. 2014.

[49] D. K. Dheer, S. Doolla, S. Bandyopadhyay, and J. M. Guerrero, "Effect of placement of droop based generators in distribution network on small signal stability margin and network loss," *Elec. Power and Energy Syst. Elsevier*, vol. 88, pp. 108-118, Jun. 2017.

[50] H. Liang, B. J. Choi, W. Zhuang, and X. Shen, "Stability enhancement of decentralized inverter control through wireless communications in microgrids," *IEEE Trans. Smart Grid*, vol. 4, no. 1, pp. 321-331, Mar. 2013.

[51] S. V. Iyer, M. N. Belur, and M. C. Chandorkar, "A generalized computational method to determine stability of a multi-inverter microgrid," *IEEE Trans. Power Electron.*, vol. 25, no. 9, pp. 2420-2432, Apr. 2010.

[52] I. P. Nikolakakos, H. H. Zeineldin, M. S. El-Moursi, and N. D. Hatziargyriou, "Stability evaluation of interconnected multi-inverter microgrids through critical clusters," *IEEE Trans. Power Syst.*, vol. 31, no. 4, pp. 3060-3072, Jul. 2016.